Numerical Identification of Time-Varying Coefficient for Pseudo-Hyperbolic Equation under Non-Local Integral Extra Condition

Anam Alwan Salih[1,2] and Mohammed Sabah Hussein[2]
[1]*Ministry of Education, General Education in Baghdad-Karkh II, Baghdad, Iraq*
[2]*Department of Mathematics, College of Science, University of Baghdad, Baghdad, Iraq*
inam.alwan2303@sc.uobaghdad.edu.iq, mmmsh@sc.uobaghdad.edu.iq

Keywords: Inverse Boundary-Value Problem, Pseudohyperbolic Equation; Additional Integral Condition, Tikhonov Regularization, Nonlinear Optimization.

Abstract: This article refers to the integral numerical analysis of the inverse boundary-value problem for a pseudohyperbolic equation, incorporating an additional integral condition. While the theoretical uniqueness of the solution has been established, the problem remains ill-posed due to its high sensitivity to small variations in the input data. To address this, the study employs the Crank-Nicolson finite difference method for both temporal and spatial discretization, combined with Tikhonov regularization to ensure the stability of the inversion process. The regularization parameter is judiciously chosen to strike an optimal balance between stability and accuracy. The resulting nonlinear minimization task is addressing MATLAB's lsqnonlin function, applied to both exact and noise-effected data sets. A Von Neumann stability analysis confirms the robustness of the numerical scheme. Computational findings reveal that the proposed method delivers precise and stable result, even in the presence of noisy data. This work marks the first practical numerical solution to this inverse problem, demonstrating the efficacy of combining finite-difference discretization with Tikhonov regularization, thereby providing a solid foundation for future numerical and applied investigations within this domain of boundary-value problems.

1 INTRODUCTION

Very large-scale models of physical and engineering problems, including wave propagation and dynamic phenomena, are modeled using hyperbolic partial differential equations (PDEs). Some of the basic processes that can be explained using these equations include sound waves, electromagnetism, and medical imaging [1].

The Klein-Gordon equation, the wave equation, and the equations governing the propagation of electromagnetic and seismic waves are prominent examples of classical hyperbolic equations. Pseudo-hyperbolic (PH) equations in a more general sense, are based on more complex generalizations of the hyperbolic behavior or dispersive action. Hyperbolic equations, more generally, are related to pseudo-hyperbolic equations, which are subjected to one further derivation or dispersion. They are more difficult to manipulate and are used to simulate phenomena such as wave behavior in non-homogeneous materials, the vibration of elastic plates, and the conduction of energy in composite materials. Consequently, pseudo-hyperbolic equations often require subsequent mathematical processing, since their dispersive and wave-like natures interact with one another, unlike in the classical hyperbolic equations [2].

The existence, uniqueness, and stability of solutions to a problem are crucial in theory, with existence being a pivotal aspect in cases involving non-local integral conditions. This is because these conditions restrict measurements to the domain (using either world-wide of measurements or averaged measurements over the domain), which is typical of real-life problems in which aggregate measurements are necessary [3]-[5]. Among these directions is the task of tackling the fourth-order pseudo-hyperbolic (PH) boundary value problem with non-local integral conditions, in which the existence and uniqueness of solutions have been proved by applying auxiliary transformations and fixed-point arguments [6].

Conversely, the paper [7] aims to tackle inverse hyperbolic and pseudo-hyperbolic (PH) equations with periodic boundary conditions, using either an analytical or a numerical approach. In a same manner, paper [8] looks at a first-order, two- dimensional hyperbolic inverse problem, with the aim of restoring a time-dependent potential term, using additional measurements, initial specification and a global constraint in the spatial space. In paper [9], the time-dependent unknown coefficients are investigated for a one-dimensional non-linear hyperbolic equation or (PH equation) with periodic boundary conditions.

Recent efforts [10] have established the existence and uniqueness of solutions to inverse boundary-value problems for hyperbolic equations with both variable and constant coefficients under specified boundary conditions. Moreover, research [11], [12] has discussed the recovery of temporally varying coefficients and evaluated their effect on the solution stability. As the challenges of directly translating standard numerical processes are pervasive, a specialized computational process is likely required for the inverse hyperbolic form of the problem.

Common methods that have been used include finite difference [13], [14], finite element [15], [16], and finite volume [17], [18] schemes, though spectral and wavelet methods have been identified as being more accurate. The chosen methodology is usually based on the nature of the problem, the boundary arrangements, and the accuracy of the input data. As a result, significant research has been done on the stabilization methods to make these inverse problems practical. In this case, the simplest method is the Tikhonov regularization, which was originally introduced in the early 1960s; it is also supplemented with several optimization methods that improve the robustness of the solution. The necessity of Tikhonov regularization in ill-posed problems of hyperbolic systems has received the attention of numerous of researchers [19].

The present work is grounded in the numerical calculation of an unknown coefficient, which is an ill-posed problem, as a slight differences in the information presented may introduce dramatic turbulence in the oscillations of the final solution. To overcome this instability and improve the consistency of the results, a stabilization methodology based on nonlinear Tikhonov regularization is adopted [18].

This paper is organized as follows. Section 2 provides the mathematical foundation of the issue being examined. Section 3 delineates the discretization scheme and elucidates the numerical solution of the direct problem (DP) using the finite difference method (FDM), which integrates the Crank-Nicolson technique with the finite difference approach. Portion 4 reports on the numerical method of finding the solution of the Inverse problem (IP), in which the response is obtained by minimizing of the objective/misfit function. The numerical experiments and discussion are presented in Section 5, while the fact that the major findings of the study are given in Section 6.

2 PROBLEM MATHEMATICAL STATEMENT

Below [20] is an example of a non-self-adjoint inverse boundary value problem with non-self-adjoint boundary conditions. The governing equation is given by:

$$w_{\tau\tau} - w_{\tau\tau xx} - w_{xx} = \beta(\tau)w(x,\tau) + s(x,\tau), (x,\tau) \in D_{t_f}\,. \quad (1)$$

Where x represents the spatial variable, while τ corresponds to time. The function $w(x,\tau)$ is the unknown displacement, $s(x,\tau)$ is a known source term representing a distributed force, and $\beta(\tau)$ is an unknown time-dependent coefficient that needs to be determined. The solution domain is specified as follows: where the solution domain is $D_{t_f} = \{(x,t): 0 \le x \le 1, 0 \le \tau \le t_f\}$,

This equation is subject to initial conditions of the form.

$$w(x,0) = \varphi(x)\,, w_t(x,0) = \psi(x)\,, (0 \le x \le 1), \quad (2)$$

and the boundary conditions:

$$w(0,\tau) = w(1,\tau), w_x(1,\tau) = 0 \;\; (0 \le t \le t_f), \quad (3)$$

along with an additional condition of the integral type

$$\int_0^1 w(x,\tau)dx = h(\tau). \quad (4)$$

It is important to note that the term $w_{\tau\tau xx}$ introduces a pseudo-behavior, which leads to a damping effect on the hyperbolic nature of the wave. The functions $s(x,\tau), \varphi(x), \psi(x)$, and $h(\tau)$ are known and predefined, while $w(x,\tau)$ and $\beta(\tau)$ are unknown functions to be determined.

Definition 1. The classical solution to the inverse boundary value problem (1)-(4) is the pair of functions $\{w(x,\tau), \beta(\tau)\}$, where $w(x,\tau) and\, \beta(\tau)$ satisfy the following properties:

1) The function $w(x,\tau)$ remains continuous within D_{t_f}, along with all its derivatives involved in (1);
2) The function $\beta(\tau)$ is continuous over the entire interval $[0, t_f]$;

3) All conditions (1)-(4) are fulfilled in the standard sense.

The following result holds.

Lemma 1. Let $s(x,\tau) \in D_T$, $\varphi(x)$, $\psi(x) \in C[0,1]$, $h(\tau) \in C^2[0,t_f], h(\tau) \neq 0$ for $\tau \in [0,t_f]$ and the following compatibility conditions hold:

$$\int_0^1 \varphi(x)\,dx = h(0), \qquad \int_0^1 \psi(x)\,dx = h'(0).$$

Consequently, ascertaining a classical solution to issue (1)-(4) is tantamount to identifying the function $w(x,\tau)$and $\beta(\tau)$, which satisfy properties (1 and (2 of the classical solution definition, derived from relations (1)-(3) and fulfilling:

$$\beta(\tau)h(\tau) + \int_0^1 s(x,\tau)\,dx = h''(\tau) + u_{\tau\tau x}(0,t) + u_x(0,\tau) \ \ (0 \le \tau \le t_f). \tag{5}$$

Proof. see [20].

Theorem 1. Assume that the given data of problem (1)-(3), (5) meet the following requirements:

1) $\varphi(x) \in C^2[0,1], \varphi(x) \in L_2(0,1), \varphi(0)=\varphi(1), \varphi'(1)=0, \varphi(0) = \varphi''(1)$.
2) $\psi(x) \in C^2[0,1], \psi(x) \in L_2(0,1), \psi(0)=\psi(1), \psi(1) = 0, \psi(0)=\psi(1)$.
3) $s(x,\tau) \in C\left(D_{t_f}\right), s_x(x,\tau) \in L_2\left(D_{t_f}\right), f(0,\tau) = f(1,\tau)(0 \le \tau \le t_f)$.
4) $h(\tau) \in C^2[0,t_f], h(\tau) \neq 0 for\ \tau \in [0,t_f]$.

Then the problem (1)-(3), (5) has a unique solution.
Proof: see [20].

Theorem 2. Assume that conditions 1-4 hold, and

$$B(t_f)\left(A(t_f)+2\right)^2 < 1 . \tag{6}$$

Then the IP (1)-(3), (5) possesses a solution in the ball $= K_R\left(\|z\|_{E^3_{t_f}} \le R = A(t_f)+2\right)$, from $E^3_{t_f}$ has a unique solution. Where:

$$A(t_f) = A_1(t_f) + A_2(t_f),$$

$$B(t_f) = B_1(t_f) + B_2(t_f),$$

And:

$$A_1(t_f) = \|\varphi(x)x\|_{L_{2(0,1)}} + t_f\|\psi(x)\|_{L_{2(0,1)}},$$

$$+4\sqrt{t_f}\|s(x,\tau)x\|_{L_2(D_{t_f})} + \sqrt{2}\left\|\varphi^{(3)}(x)\right\|_{L_{2(0,1)}},$$

$$+2[\![\psi^3(x)]\!]_{L_{2(0,1)}} + 2\sqrt{T}\|s_x(x,\tau)\|_{L_2(D_{t_f})},$$

$$+\sqrt{5}\left\|\varphi^{(3)}(x)+\varphi^{(2)}(x)\right\|_{L_{2(0,1)}} + \sqrt{10}\left\|\psi^{(3)}(x) + \psi^{(2)}(x)\right\|_{L_{2(0,1)}} + 2\sqrt{5}(t_f+1)\|s_x(x,\tau) + s(x,\tau)\|_{L_2(D_T)} + \sqrt{10}t_f[\![\varphi(x)]\!]_{L_{2(0,1)}} + (\sqrt{2}+t_f)\sqrt{20}\|\psi(x)\|_{L_{2(0,1)}} + 2\sqrt{10t_f}(t_f+1)\|s(x,\tau)\|_{L_2(D_{t_f})},$$

$$B_1(t_f) = (t_f)^2 + 2\sqrt{2}t_f + 2\sqrt{10}t_f(t_f+1) .$$

$$A_2(t_f) = \|h^{-1}(\tau)\|_{C[0,T]}\left\{\left\|h''(\tau) - \int_0^1 s(x,\tau)dx\right\|_{C[0,1]} + 4\left[\sum_{k=1}^{\infty}\lambda_k^{-2}\right]^{1/2}\left[\|\varphi(x)\|_{L_{2(0,1)}} + \sqrt{2}\|\psi(x)\|_{L_{2(0,1)}} + \sqrt{2t_f}\|f(x,\tau)\|_{L_2(D_{t_f})} + \left\|\|s(x,\tau)\|_{C[0,t_f]}\right\|_{L_{2(0,1)}}\right]\right\},$$

$$B_2(t_f) = \|h^{-1}(\tau)\|_{C[0,t_f]}\left(\sum_{k=1}^{\infty}\lambda_k^{-2}\right)^{1/2}(2t_f+1).$$

Proof: see [20].

Theorem 3. Let all the conditions of Theorem 2 be satisfied, and

$$\int_0^1 \varphi(x)dx = h(0), \int_0^1 \psi(x)dx = h'(0).$$

Hence, the IP (1)-(4) admits a solution within the ball $K = K_R\left(\|z\|_{E^3_{t_f}} \le R = A(t_f)+2\right)$ from $E^3_{t_f}$ has only classical solution.

Proof: see [20].

3 CRANK-NICOLSON FDM DISCRETIZATION OF THE DP (1)-(3)

We investigate the direct initial-boundary value issue delineated by equations (1)-(3), whereby the functions $\beta(\tau), \varphi(x), \psi(x)$ and $s(x,\tau)$ are known, and the objective is to determine $w(x,\tau)$.

We denote; $w(x_i,\tau_j) = w_{i,j}$, $\beta(\tau_j) = \beta_j$, and $s(x_i,\tau_j) = s_{i,j}$ where, the space node is $x_i = ih$ and the time node is $\tau_j = jk$, while the space and time step length are $h = \frac{1}{M}$ and $k = \frac{t_f}{N}$, for $i = \overline{0,M}$, $j = \overline{0,N}$, where M and N are positive integer.

The Crank-Nicolson FDM [21], [22], which is unconditionally stable, can then be used to discretize (1) as follows:

$$\frac{w_{i,j+1}-2w_{i,j}+w_{i,j-1}}{k^2}-\frac{1}{h^2k^2}\left[w_{i-1,j+1}-2w_{i,j+1}+w_{i+1,j+1}-2w_{i-1,j}+4w_{i,j}-2w_{i+1,j}+w_{i-1,j-1}-2w_{i,j-1}+w_{i+1,j-1}\right]-\frac{1}{2h^2}\left[w_{i+1,j+1}-2w_{i,j+1}+w_{i+1,j+1}+w_{i-1,j}-2w_{i,j}+w_{i+1,j}\right]=\frac{1}{2}\beta_{j+1}w_{i,j+1}+\frac{1}{2}\beta_j w_{i,j}+s_{i,j,} \quad (7)$$

Rearranging the terms in the last equation yields:

$$[-E_1-E_2]w_{i-1,j+1}+\gamma_{j+1}w_{i,j+1}+[-E_1-E_2]w_{i+1,j+1}=[-2E_1+E_2]w_{i-1,j}+C_j w_{i,j}+[-2E_1+E_2]w_{i+1,j}+E_1 w_{i-1,j-1}-(1+2E_1)w_{i,j-1}+E_1 w_{i+1,j-1}+k^2 f_{i,j,} \quad (8)$$

Where:

$$E_1=\frac{1}{h^2}\,, E_2=\frac{k^2}{2h^2}\,,$$

$$\gamma_{j+1}=1+2A_1+2A_2-\frac{1}{2}\beta_{j+1}k^2\,,$$

$$C_j=2+4A_1-2A_2+\frac{1}{2}\beta_j k^2,\ \ j=0,\dots,N$$

The initial conditions are approximated as:

$$w_{i,0}=\varphi(x_i),\ \ i=\overline{0,M}, \quad (9)$$

$$w_{i,-1}=w_{i,1}-2k\psi(x_i),\ \ i=\overline{0,M}. \quad (10)$$

and the boundary conditions are also approximated as:

$$w_{0,j}=w_{M,j},\ j=\overline{0,N} \quad (11)$$

$$w_{M+1}=w_{M-1},\ j=\overline{0,N} \quad (12)$$

Given that the trapezoidal rule is used to estimate the value of the integral (4), we can obtain the following expression;

$$h(\tau_j)=\int_0^1 w(x,\tau_j)\,dx=\frac{h}{2}\Big(w_{0,j}+w_{M,j}+2\sum_{i=1}^{M-1}w(x_i,\tau_j)\Big),\ \ j=\overline{0,N}\,. \quad (13)$$

The discretize system (8)-(13) can be break down into two-level time scheme as following;

With $j=0$, (8) can be expressed as follows:

$$[-E_1-E_2]w_{i-1,1}+\gamma_1 w_{i,1}+[-E_1-E_2]w_{i+1,1}=[-2E_1+E_2]w_{i-1,0}+C_0 w_{i,0}+[-2E_1+E_2]w_{i+1,0}+E_1 w_{i-1,-1}-(1+2E_1)w_{i,-1}+E_1 w_{i+1,-1}+k^2 s_{i,0}\,, \quad (14)$$

- For space index $i=0$, it comes from (14), which equals zero.
- For space index $i=1$, substituting condition (10) into (14), we get the following result:

$$[-2E_1-E_2]w_{0,1}+[1+2E_1+\gamma_1]w_{1,1}+[-2E_1-E_2]w_{2,1}=[-2E_1+E_2]w_{0,0}+C_0 w_{1,0}+[-2E_1+E_2]w_{2,0}-2k[E_1\psi(x_0)-(1+2E_1)\psi(x_1)+E_1\psi(x_2)]+k^2 s_{1,0}, \quad (15)$$

For space index $i=M+1$, substituting conditions (10) and (12) into (14), we have:

$$[-4E_1-2E_2]w_{M,1}+[1+2E_1+\gamma_1]w_{M+1,1}=[-4E_1+2E_2]w_{M,0}+C_0 w_{M+1,0}-2k[2E_1\psi(x_M)-(1+2E_1)\psi(x_{M+1})]+k^2 s_{M+1,0}, \quad (16)$$

The above (14)-(16) can be expressed as an $(M+1)\times(M+1)$ linear system of algebraic equations in two-time levels;

$$LU_1=DU_0+Z+F\,. \quad (17)$$

$$\mathrm{L}=\begin{cases} 1+2\mathrm{E}_1+\gamma_1, & \text{for main digonal entries} \\ -2\mathrm{E}_1-\mathrm{E}_2, & \text{for upper and lower digonal entries} \\ -4\mathrm{E}_1-2\mathrm{E}_2, & \text{for the entry at postion } (\mathrm{M},\mathrm{M}+1) \\ 0, & \text{otherwise} \end{cases}$$

$$D=\begin{cases} \mathrm{C}_0 & \text{for main digonal entries} \\ 2\mathrm{E}_1+\mathrm{E}_2 & \text{for upper and lower digonal entries} \\ 2(-2\mathrm{E}_1+\mathrm{E}_2) & \text{for the entry at postion } (\mathrm{M},\mathrm{M}+1) \\ 0, & \text{otherwise} \end{cases}$$

$$Z=-2k\begin{bmatrix} 0 \\ E_1\psi(x_0)-(1+2E_1)\psi(x_1)+E_1\psi(x_2) \\ E_1\psi(x_1)-(1+2E_1)\psi(x_2)+E_1\psi(x_3) \\ \vdots \\ E_1\psi(x_{M-1})-(1+2E_1)\psi(x_M)+E_1\psi(x_{M+1}) \\ E_1\psi(x_M)-(1+2E_1)\psi(x_{M+1}) \end{bmatrix}_{(M+1)\times 1},$$

$$F=\begin{bmatrix} 0 \\ s_{1,0} \\ s_{2,0} \\ \vdots \\ s_{M,0} \\ s_{M+1,0} \end{bmatrix}_{(M+1)\times 1}.$$

In the context, $\mathrm{W}_1=(\mathrm{w}_{0,1},\mathrm{w}_{1,1},\dots,\mathrm{w}_{M+1,1})^{\mathrm{T}}$ and $\mathrm{W}_0=(\mathrm{w}_{0,0},\mathrm{w}_{1,0},\dots,\mathrm{w}_{M+1,0})^{\mathrm{T}}$ denote the solution vectors evaluate at times τ_1 and τ_0 respectively.

- Now, for the rest of the nodes, i.e., $\mathrm{j}=1,2,\dots,\mathrm{N}$, then (8) becomes as follows:

$$[-\mathrm{E}_1-\mathrm{E}_2]\mathrm{w}_{i-1,j+1}+\gamma_2\mathrm{w}_{i,j+1}+[-\mathrm{E}_1-\mathrm{E}_2]\mathrm{w}_{i+1,j+1}=[-2\mathrm{E}_1+\mathrm{E}_2]\mathrm{w}_{i-1,j}+\mathrm{C}_1\mathrm{w}_{i,j}+ \quad (18)$$

$[-2E_1 + E_2]w_{i+1,j} + E_1 w_{i-1,j-1} - (1 + 2E_1)w_{i,j-1} + E_1 w_{i+1,j-1} + k^2 s_{i,j}$,

- For $i = 1$, (18) leads to the following:

$$[-E_1 - E_2]w_{0,2} + \gamma_2 w_{1,2} + [-E_1 - E_2]w_{2,2} = [-2E_1 + E_2]w_{0,1} + C_1 w_{1,1} + [-2E_1 + E_2]w_{2,1} + A_1 w_{0,0} - (1 + 2E_1)w_{1,0} + E_1 w_{2,0} + k^2 s_{1,1} \quad (19)$$

At the end grid point $i = M + 1$, by applying condition (12) to (18), we obtain:

$$[-2E_1 - 2E_2]w_{M,2} + \gamma_2 w_{M+1,2} = [-4E_1 + 2E_2]w_{M,1} + C_1 w_{M+1,1} + 2E_1 w_{M,0} - (1 + 2E_1)w_{M+1,0} + k^2 s_{M+1,1}, \quad (20)$$

As a result, (18)-(20) can be expressed as a system of linear algebraic equations.

$$L_1 U_{j+1} = D_1 U_j + Z_1 U_{j-1} + F_1. \quad (21)$$

$$L_1 = \begin{cases} \gamma_2 \text{ for main digonal entries} \\ -E_1 - E_2 \text{ for upper and lower digonal entries} \\ 2[-E_1 - E_2] \text{ forthe entry at postion } (M, M+1) \\ 0, \quad \text{otherwise} \end{cases}$$

$$D_1 = \begin{cases} C_1 \text{ for main digonal entries} \\ -2E_1 + E_2 \text{ for upper and lower digonal entries} \\ 2[-2E_1 + E_2] \text{ for the entry at postion } (M, M+1) \\ 0, \quad \text{otherwise} \end{cases}$$

$$Z_1 = \begin{bmatrix} 0 & 0 & 0 \dots & 0 & 0 & 0 \\ E_1 & -(1+E_1) & E_1 & 0 & 0 & 0 \\ 0 & E_1 & -(1+E_1) & E_1 & 0 & 0 \\ \vdots & \vdots & \vdots & \vdots & \vdots & \vdots \\ 0 & 0 & 0 & E_1 & -(1+E_1) & E_1 \\ 0 & 0 & 0 & 0 & 2E_1 & -(1+E_1) \end{bmatrix}_{((M+1)\times(M+1)}$$

$$F_1 = \begin{bmatrix} 0 \\ s_{1,1} \\ s_{2,1} \\ \vdots \\ s_{M,1} \\ s_{M+1,0} \end{bmatrix}_{(M+1)\times 1}.$$

Here, $W_{j+1} = \left(w_{0,j+1}, w_{1,j+1}, \dots, w_{M+1,j+1}\right)^T$, represent the solution vectors, while L_1, D_1 andZ_1 are tridiagonal matrices.

3.1 Stability analysis of the DP (1)-(3)

Employing the Von Neumann method [23], [24] to prove the stability of scheme (8). Let U be the exact solution of (8), and $\tilde{U}$ denote the numerical solution. Define the error $E = \tilde{z} - z$,

$$\tilde{E}_j = \tilde{z}_j - z_j = \left(e_{0,j}, e_{1,j}, \dots, e_{M,j}\right)$$

i.e. $e_{i,j} = \tilde{z}_{i,j} - z_{i,j}$ then $s_{i,j} = 0$, $i = \overline{0, M}$, $j = \overline{0, N}$

Now, consider Fourier mode $e_{i,j} = S^j e^{i\omega\theta}$, where i represents the node number, $\omega = \sqrt{-1}$, and θ is the phase angle, and assuming a constant local value $\beta_j = \beta_{j+1} = b$ for a known level in (8), where $b = \max_{\tau\in[0,t_f]} |\beta(\tau)|$, we obtain the following expression:

$$[-E_1 - E_2]e_{i-1,j+1} + \gamma e_{i,j+1} + [-E_1 - E_2]e_{i+1,j+1} = [-2E_1 + E_2]e_{i-1,j} + Ce_{i,j} + [-2E_1 + E_2]e_{i+1,j+1} + E_1 e_{i-1,j-1} - (1 + 2E_1)e_{i,j-1} + E_1 e_{i+1,j-1} \quad (22)$$

By substituting the Fourier mode into (22) and simplifying the resulting terms, we obtain;

$$[2(-E_1 - E_2)\cos\theta + \gamma]S^2 - [2(-2E_1 + E_2)\cos\theta + C]S + \left[4E_1 \sin^2\left(\frac{\theta}{2}\right) + 1\right] = 0 \quad (23)$$

which can be reformulated as;

$$PS^2 - QS + R = 0, \quad (24)$$

where,

$$P = 2(-E_1 - E_2)\cos\theta + \gamma, \; Q = 2(-2E_1 + E_2)\cos\theta + C,$$

$$R = 4E_1 \sin^2\left(\frac{\theta}{2}\right) + 1 .$$

Under the transformation $S = \frac{1+\rho}{1-\rho}$ introduced in (24), we obtain

$$(P + Q + R)\rho^2 + 2(P - R)\rho + (P - Q + R) = 0, \quad (25)$$

The system described by (23) is stable if and only if the condition $|S| \leq 1$ is satisfied and

$$P + Q + R \geq 0, \; P - R \geq 0, \text{ and } P - Q + R \geq 0 \quad (26)$$

Replacing the values of P, Q, and R and simplifying the resultant terms, we end up with:

$$P + Q + R = 4 + 16E_1 \sin^2\left(\frac{\theta}{2}\right) \geq 0, \quad (27)$$

$$P - R = 4E_1 \sin^2\left(\frac{\theta}{2}\right) + 4E_2 \sin^2\left(\frac{\theta}{2}\right) - \frac{1}{2}bk^2, \quad (28)$$

$$P - Q + R = 8E_1 \sin^2\left(\frac{\theta}{2}\right) - bk^2. \quad (29)$$

Since the phase angle is given by $= \pi h = \frac{\pi}{M}$, it follows that $P - R \geq 0$ and $P - Q + R \geq 0$ when $h \leq 2\frac{1}{\sqrt{b}}\sin\left(\frac{\pi h}{2}\right)$. Therefore, the discretized system for the Boussinesq-Love equation will exhibit stability.

3.2 Example for DP (1)-(3)

We aimed to evaluate the robustness and effectiveness of the proposed Crank-Nicolson FDM method for solving the direct problem, considering scenarios where the unknown coefficient is known beforehand.

$$\varphi(x) = x^2(1-x)^2 + 1,$$

$$\psi(x) = -2[x^2(1-x)^2 + 1], x \in [0,1]$$

$$\beta(\tau) = \cos(4\pi\tau) - |\tau - 0.01|, \tau \in [0, t_f = 1]$$

$$s(x,\tau) = e^{-2\tau}[-6 + 60x - 56x^2 - 8x^3 + 4x^4(1 + x^2 - 2x^3 + x^4)]|\tau - 0.01| - (1 + x^2 - 2x^3 + x^4)\cos(4\pi\tau), \ (x,\tau) \in D_{t_f}$$

Along with the integral condition, extra data The exact solution is;

$$w(x,\tau) = e^{-2\tau}[x^2(1-x)^2 + 1], (x,\tau) \in D_{t_f}$$

The solution may be checked by simply replacing it in the governing equation (1). The exact and computed values of $w(x,\tau)$ at $M = N = 100$ mesh are plotted in Figure 1, and the degree of accuracy is very high, as seen in the plot of the error, which has an error magnitude on the same order of 10^{-4}. The calculated value of $h(\tau)$ and the analytical result are shown in Figure 2, which shows that the two values are in great agreement.

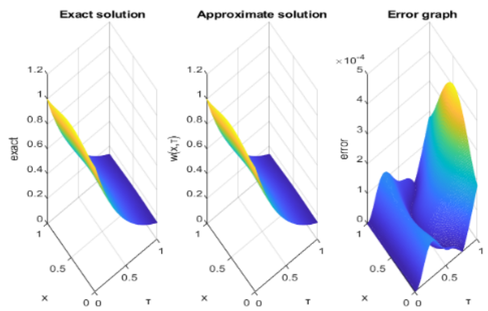

Figure 1: Comparison of the exact and approximate solution $w(x,\tau)$ and their error over the domain D_{t_f}.

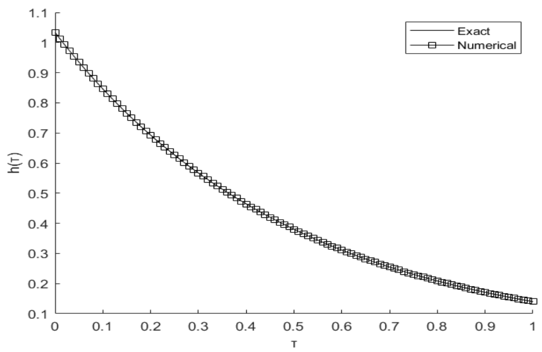

Figure 2: Exact and numerical solutions $h(\tau)$ over time, showing good agreement.

4 NUMERICAL APPROACHES FOR SOLVING IP (1)-(4)

4.1 Formulation of the Regularized Optimization Problem

The numerical solution of the inverse problem (1)-(4) is formulated as a nonlinear optimization task. Specifically, the unknown coefficient $\beta(\tau)$ is obtained by minimizing the following Tikhonov-regularized cost functional:

$$\Gamma(\beta) = \sum_{j=1}^{N} \left(\int_0^1 w(x_i,\tau_j)dx - h(\tau_j)^2\right)^2 + \lambda \sum_{j=1}^{N} \beta_j^2, \quad (30)$$

where $\lambda \geq 0$ is the regularization parameter, which is introduced to ensure the stability of the solution.

To approximate $\beta(\tau)$, the function $w(x,\tau)$ is determined by solving the direct problem (1)-(3) using the Crank-Nicolson finite difference method. The regularization parameter λ is selected through a trail-and-error strategy to achieve an optimal balance between solution stability and accuracy. Standard methods for parameter selection, such as the L-curve method, is not applicable in this context due to the nonlinear nature of the inverse problem; thus, making trial-and-error approach a practical and reliable alternative [25].

The minimization of the functional $\Gamma(\beta)$ is performed using MATLAB's lsqnonlin function, which iteratively solves nonlinear least square problems starting from an initial guess. The unknown parameter β is constrained within the bounded $10^{-3} \leq \beta \leq 10^3$. The trust-region reflective algorithm, based on the interior-reflective Newton method, is employed to efficiently optimize the solution, for more details see, [26]

To assess the method's robustness, the inverse problem is solved employing both precise and noisy data. The noisy measurement is generated as

$$\|h^\varepsilon - h\| \leq \varepsilon, \quad (31)$$

where ε is a random variable following a Gaussian distribution with zero mean and standard deviation σ, defined by

$$\sigma = p \times \max_{\tau\in[0,t_f]} |h(\tau)|, \quad (32)$$

For the noisy case, the function h in (30) is replaced by h^ε.

4.2 Determination of the Initial Guess for the Coefficient $\boldsymbol{\beta}$

In the minimization process, we require an initial guess. Thus, applying equation (1) with the space variable as the variable of integration, we obtain,

$$\int_0^1 w_{\tau\tau} dx - \int_0^1 w_{\tau\tau xx} dx - \int_0^1 w_{xx} dx = \beta(\tau) \int_0^1 w(x,\tau) + \int_0^1 s(x,\tau)\, dx,$$

since $\int_0^1 w(x,\tau)\, dx = h(\tau)$, we have

$$\int_0^1 w_{\tau\tau}\, dx - \int_0^1 w_{\tau\tau xx}\, dx - \int_0^1 w_{xx}\, dx = \beta(\tau)h(\tau) + \int_0^1 s(x,\tau)\, dx\ ,$$

$$\int_0^1 w_{\tau\tau}\,(x,\tau)dx - w_{\tau\tau x}(x,\tau)|_0^1 - w_x|_0^1 = \beta(\tau)h(\tau) + \int_0^1 s(x,\tau)dx\ ,$$

$$\int_0^1 w_{\tau\tau}(x,\tau)dx - [w_{\tau\tau x}(1,\tau) - w_{\tau\tau x}(0,\tau)] - [w_{\ x}(1,\tau) - w_x(0,\tau)] = \beta(\tau)h(\tau) + \int_0^1 s(x,\tau)\, dx.$$

By using boundary condition (3), the last equation becomes;

$$\int_0^1 w_{\ \tau\tau}(x,\tau)dx - \left[\frac{\partial^2}{\partial\tau^2}\big(w_x(1,\tau)\big) - \frac{\partial^2}{\partial\tau^2}\big(w_x(0,\tau)\big)\right] + w_x(0,\tau) = \beta(\tau)h(\tau) + \int_0^1 s(x,\tau)dx\ ,$$

that is,

$$\int_0^1 w_{\tau\tau}(x,\tau)\, dx + \frac{\partial^2}{\partial\tau^2} w_x(0,\tau) + w_x(0,\tau) - \int_0^1 s(x,\tau)dx = \beta(\tau)h(\tau),$$

evaluating equation at $\tau = 0$, we have

$$\int_0^1 w_{\ \tau\tau}(x,\tau)\, dx + \frac{\partial^2}{\partial\tau^2}\big(w_{\ x}\,(0,\tau)\big)\,|_{\,\tau=0} + \varphi'(0) - \int_0^1 s(x,\tau)dx = \beta(0)h(0),$$

$$\beta(0) = \frac{1}{h(0)}\left[\int_0^1 w_{\tau\tau}(x,\tau)\, dx + w_{\tau\tau x}(0,\tau)\,|_{\,\tau=0} + \varphi'(0) - \int_0^1 s(x,\tau)dx\right].$$

5 RESULTS AND DISCUSSION

In this section, we conduct a few numerical experiments to verify the accuracy of the retrieved coefficient and ensure the consistency of the obtained numerical results.

It is a hybrid approach that combines Crank-Nicolson FDM as a direct solver, presented in Section 3, with the minimization of the objective functional, presented in Section 5. This combination allows us to achieve the desired output by finding the minimum of the point representing the objective functional. Additionally, the input measurement conditions are subject to noise, as specified by equation (30). To assess the precision of the numerical outputs, the root mean square error (RMSE) is calculated using the following formula:

$$RMSE(\beta) = \left[\frac{T}{N}\sum_{j=1}^{N}\big(\beta^{Numerical}(\tau_j) - \beta^{exact}(\tau_j)\big)^2\right]^{1/2}. \quad (33)$$

In both following examples, the final time is fixed at $\mathrm{t_f} = 1$ for simplicity.

Example 5.1. Here, we investigated the behavior of a smooth function $\beta(\tau)$. This nonlinear function is what we aim to recover. Consequently, we assume the following information for the inverse problem (1)-(4):

$$\varphi(x) = \cos(2\pi x) + 1, \quad x \in [0,1]$$

$$\psi(x) = -[\cos(2\pi x) + 1], \;\; x \in [0,1]$$

$$s(x,\tau) = e^{-t}[-\sin(6\pi\tau) - \cos 2\pi x\,(-8\pi^2 + \sin(6\pi\tau)], \qquad (x,\tau) \in D_{t_f}$$

and $\mathrm{h}(\tau)$, whilst the true solution to this problem is given by $(\mathrm{w}(\mathrm{x},\tau), \beta(\tau)) = (\mathrm{e}^{-t}(\cos(2\pi x) + 1), \sin(6\pi\tau) + 1)$,

In this study, we initialize the first guess for $\beta(0)=1$ and employ a range of mesh sizes, specifically $M=N\in\{10,20,40,60\}$. We commence with the instance of the perfect data, where $\mathrm{p} = 0$.

The misfit function (30) is informed to approach a very small minimum of order $O(10^{-10})$ and approaches it monotonically and rapidly in about 10 iterations, as indicated in Figure 3. Figure 4 shows the associated numerical results of the potential $\beta(\tau)$. Table 1 reveals that the RMSE (β) is associated with the various mesh sizes. These results demonstrate efficient and stable convergence under noise-free conditions, with high numerical accuracy reflected by the very small misfit. The consistency of RMSE (β) a cross-mesh sizes indicates acceptable stability of the method, although further validation with noisy data is still required.

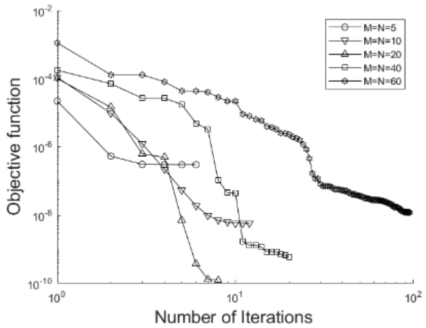

Figure 3: Misfit function (30) plotted against the number of iterations for different mesh sizes, in the absence of noise and without regularization, for Example 5.1.

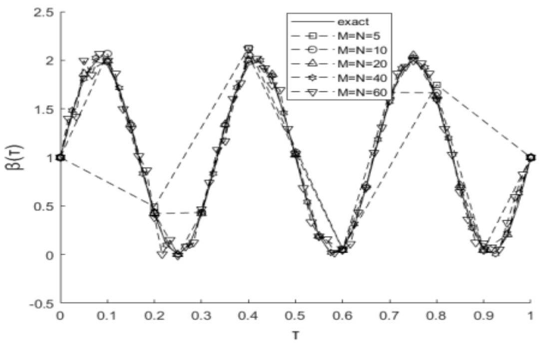

Figure 4: Comparison between exact and numerical solution of $\beta(\tau)$ in the noise-free case without regularization, using mesh sizes $M = N \in \{5,10,20,40,60\}$, for Example 5.1.

Table 1: The RMSE (β) values for mesh sizes $M = N \in \{5,10,20,40,60\}$ in Example 5.1.

M=N	5	10	20	40	60
rmse(a)	0.1130	0.0625	0.0309	0.0254	0.0808

Subsequently, we investigated the numerical reconstruction stability in the presence of small portions of noise in the input information, denoted as $h(\tau)$. Specifically, we examined the stability for $p \in \{0.01\%, 0.1\%\}$. Higher noise levels were also considered in (32), but the retrievals exhibited minimal accuracy and are therefore not reported.

The numerical results for $\beta(\tau)$ are shown in Figure 5a, b. As observed, the solutions are unstable and inaccurate, indicating that the inverse problem is highly sensitive when no regularization is applied ($\lambda = 0$), with $\mathrm{RMSE}(\beta) = 0.2912$ at $p = 0.01\%$ and $\mathrm{RMSE}(\beta) = 9.4579$. These findings underscore the necessity of regularization to obtain accurate and stable solutions. Figure 6a, b illustrates that the objective function converges monotonically in a decreasing manner. This demonstrates that even minute levels of noise can significantly impact the reconstruction process, thereby confirming that the problem is ill-posed without the application of regularization.

Regularization was applied using $\lambda \in \{10^{-6}, 10^{-7}, 10^{-8}, 10^{-9}\}$, and Figure 7 representing $\beta(\tau)$ shows the results, which indicate the presence of an oscillatory and unstable behavior of the solution. Indicating how the choice of the regularization parameter affects the amplitude and pattern of $\beta(\tau)$ and the overall stability of the reconstruction. Figure 8 also shows that the objective function (30) converged throughout the iterative optimization process in various regularization parameters. It is noted that the misfit function diminishes quickly in the iterations and then flattens to a near constant value, which is an indication of rapid and steady convergence of the suggested method.

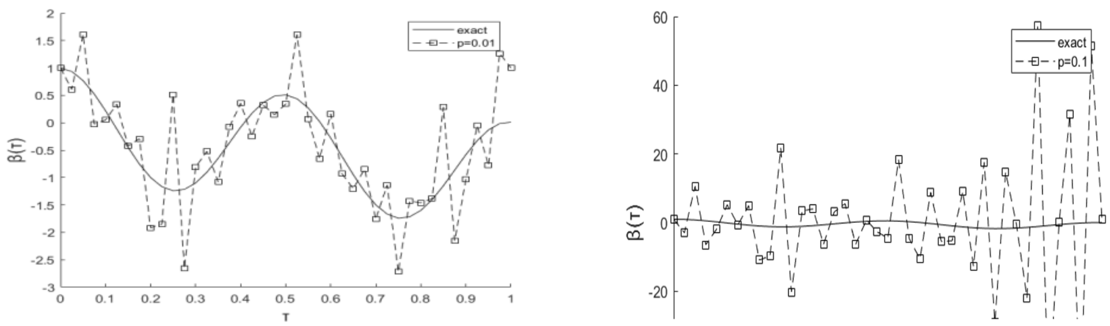

a) b)

Figure 5: The analytical and approximate recovery for $\beta(\tau)$ are shown: a) for p=0.01%, and b) p=0.1% without regularization.

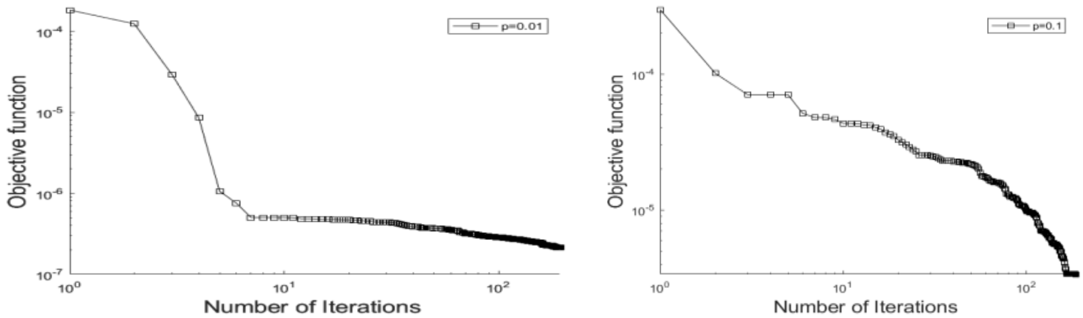

(a) (b)

Figure 6: Objective function (30) for noise level: a) p=0.01% and, b) for p=0.1% presented in both cases without regularization.

Table 2 presents the count of iterations, the quantity of function evaluations, and the ideal value of the objective function (30), to complete the RMSE (β) (32), and the computational time. Lastly, the error in the answer in the numerical solution of the equation and the exact solution of the equation $w(x,\tau)$ presented in Figure 9 for the case $(p,\lambda) = (0.01\%, 10^{-\lambda})$, a stable and oscillation-free solution is obtained.

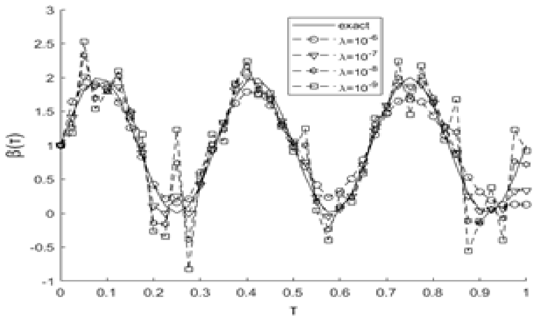

Figure 7: Comparison of the exact and approximate recovery of $\beta(\tau)$ with various regularization parameters $\lambda \in \{10^{-6}, 10^{-7}, 10^{-8}, 10^{-9}\}$.

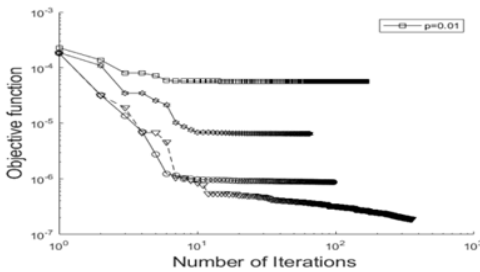

Figure 8: Objective function (30) with p=0.01% and $\lambda \in \{10^{-6}, 10^{-7}, 10^{-8}, 10^{-9}\}$.

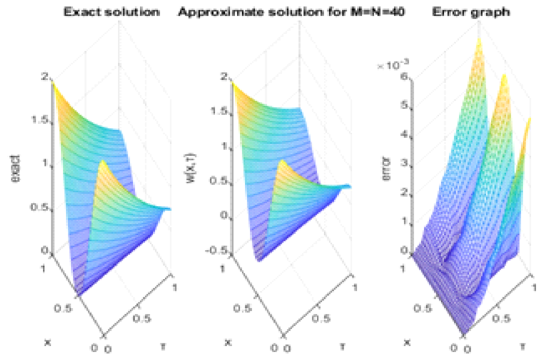

Figure 9: Comparison of the numerical and exact solution of $w(x,\tau)$ obtained using $\lambda = 10^{-7}$ with noise level p=0.01% for Example 5.1.

For example 5.1.

Table 2: A summary of the optimization outcomes for p=0.01%, reporting the iteration count to reach convergence, the number of function evaluations at the final iteration, the misfit function (30), at the termination iteration, and the total computational time consumed (in seconds).

λ	10^{-6}	10^{-7}	10^{-8}	10^{-9}
Number of iterations	165	65	96	356
Number of function evaluations	6972	2772	4074	14994
Values of objective function	5.7E-05	6.5E-06	8.7E-07	1.9E-07
$rmse(\beta)$	0.2209	0.1564	0.2735	0.4631
Computational time	27.0922	14.2313	20.8191	55.3734

6 CONCLUSIONS

In this study, a numerical approach was developed for solving an ill-posed inverse boundary-value problem for a pseudohyperbolic equation with an additional integral condition. The proposed framework combines the Crank–Nicolson finite difference discretization for the direct problem with Tikhonov regularization and a nonlinear optimization procedure for the reconstruction of the unknown coefficient.

The numerical experiments demonstrated that the proposed method provides accurate recovery of the unknown coefficient under noise-free conditions, with rapid convergence of the objective functional and stable behavior for different spatial and temporal discretizations. The obtained results also confirmed the high sensitivity of the inverse problem to perturbations in the input data, where even small levels of noise significantly affected the reconstructed solution when regularization was not applied.

The introduction of Tikhonov regularization improved the stability of the reconstruction process and reduced the influence of data perturbations. The numerical tests with different regularization parameters showed that the choice of λ plays an essential role in achieving a compromise between accuracy and stability. An appropriate regularization parameter allows the method to obtain reliable solutions while maintaining acceptable computational efficiency.

The stability analysis and numerical simulations confirm the robustness of the proposed computational scheme and demonstrate its capability for handling inverse problems governed by higher-order pseudohyperbolic equations. The presented approach can serve as a useful framework for further studies involving more complex models, multidimensional problems, and advanced parameter-selection strategies for regularization.

REFERENCES

[1] E. Alhazzani and S. Mesloub, "On a non-local initial boundary value problem for a semi-linear pseudo-hyperbolic equation in the theory of vibration," Math., vol. 11, no. 23, Art. p. 4803, 2023, [Online]. Available: https://doi.org/10.3390/math11234803.

[2] D. Serikbaev and N. Tokmagambetov, "Determination of initial data in the time-fractional pseudo-hyperbolic equation," Symmetry, vol. 16, no. 10, Art. p. 1332, 2024, [Online]. Available: https://doi.org/10.3390/sym16101332.

[3] S. Aitzhanov, J. Ferreira, and K. Zhalgassova, "Solvability of the inverse problem for the pseudohyperbolic equation," J. Math. Mech. Comput. Sci., vol. 115, no. 3, pp. 3-15, 2022, [Online]. Available: https://doi.org/10.26577/JMMCS.2022.v115.i3.01.

[4] R. Chapko and L. Mindrinos, "On the numerical solution of a hyperbolic inverse boundary value problem in bounded domains," Math., vol. 10, no. 5, Art. p. 750, 2022, [Online]. Available: https://doi.org/10.3390/math10050750.

[5] Z. S. Aliyev, Y. T. Mehraliyev, and E. H. Yusifova, "On some nonlocal inverse boundary problem for partial differential equations of third order," Turk. J. Math., vol. 45, no. 4, pp. 1871-1886, 2021, [Online]. Available: https://doi.org/10.3906/mat-2101-37.

[6] Y. Mehreliyev and A. Mammedov, "Inverse boundary value problem for fourth-order pseudo-hyperbolic equation with nonlocal integral conditions of the second kind," Eur. J. Pure Appl. Math., vol. 18, no. 2, pp. 6119-6119, 2025, [Online]. Available: https://doi.org/10.29020/nybg.ejpam.v18i2.6119.

[7] İ. Bağlan et al., "Analysis of inverse problem for pseudo-hyperbolic equation under periodic boundary condition," Sci. Rep., vol. 15, no. 1, Art. p. 41218, 2025, [Online]. Available: https://doi.org/10.1038/s41598-025-25105-1.

[8] S. Gani and M. S. Hussein, "Numerical identification of timewise dependent coefficient in hyperbolic inverse problem," Adv. Theory Nonlinear Anal. Appl., vol. 7, no. 4, pp. 148-169, 2023, [Online]. Available: https://doi.org/10.17762/atnaa.v7.i4.290.

[9] A. Yernazar, E. Aslan, and İ. Bağlan, "The dependency of the analytical and numerical solution on the ε parameter in hyperbolic and pseudo-hyperbolic problems with inverse coefficients," Commun. Fac. Sci. Univ. Ank. Ser. A1 Math. Stat., vol. 73, no. 4, pp. 1171-1196, 2024, [Online]. Available: https://doi.org/10.31801/cfsuasmas.1475286.

[10] I. Tekin, "Existence and uniqueness of an inverse problem for a second order hyperbolic equation," Univ. J. Math. Appl., vol. 1, no. 3, pp. 178-185, 2018, [Online]. Available: https://doi.org/10.32323/ujma.439662.

[11] I. Ben Aïcha et al., "Uniqueness for time-dependent inverse problems with single dynamical data," J. Math. Anal. Appl., vol. 497, no. 2, Art. p. 124910, 2021, [Online]. Available: https://doi.org/10.1016/j.jmaa.2020.124910.

[12] M. J. Huntul, M. Abbas, and D. Baleanu, "An inverse problem of reconstructing the time-dependent coefficient in a one-dimensional hyperbolic equation," Adv. Differ. Equ., vol. 2021, no. 1, Art. p. 452, 2021, [Online]. Available: https://doi.org/10.1186/s13662-021-03608-1.

[13] P. K. Abbassi et al., "Numerical solution of nonlinear partial differential equations using shifted Legendre collocation method," Bound. Value Probl., vol. 2024, no. 1, Art. p. 140, 2024, [Online]. Available: https://doi.org/10.1186/s13661-024-01933-4.

[14] V. G. Dmitriev et al., "Numerical analysis of deformation characteristics of elastic inhomogeneous rotational shells at arbitrary displacements and rotation angles," Computation, vol. 10, no. 10, Art. p. 184, 2022, [Online]. Available: https://doi.org/10.3390/computation10100184.

[15] B. Benim, A. Cemal, and W. Zinser, "Investigation into the finite element analysis of confined turbulent flows using a κ-ε model of turbulence," Comput. Methods Appl. Mech. Eng., vol. 51, no. 1-3, pp. 507-523, 1985, [Online]. Available: https://doi.org/10.1016/0045-7825(85)90045-3.

[16] L. Beilina, "Domain decomposition finite element/finite difference method for the conductivity reconstruction in a hyperbolic equation," Commun. Nonlinear Sci. Numer. Simul., vol. 37, pp. 222-237, 2016, [Online]. Available: https://doi.org/10.1016/j.cnsns.2016.01.016.

[17] D. Calvetti and E. Somersalo, "Distributed Tikhonov regularization for ill-posed inverse problems from a Bayesian perspective," Comput. Optim. Appl., vol. 91, no. 2, pp. 541-572, 2025, [Online]. Available: https://doi.org/10.1007/s10589-025-00675-y.

[18] A. Gholami and S. Gazzola, "Robust estimation of structural orientation parameters and 2D/3D local anisotropic Tikhonov regularization," Geophysics, vol. 89, no. 6, pp. V521-V536, 2024, [Online]. Available: https://doi.org/10.1190/geo2023-0632.1.

[19] M. Qassim and M. S. Hussein, "Numerical solution to recover time-dependent coefficient and free boundary from nonlocal and Stefan type overdetermination conditions in heat equation," Iraq. J. Sci., pp. 950-960, 2021, [Online]. Available: https://doi.org/10.24996/ijs.2021.62.3.25.

[20] Y. T. Mehraliev, "On the issue of solubility of one boundary-value problem for a pseudohyperbolic quartic with an additional integral condition," Univ. Proc. Volga Reg. Phys. Math. Sci., vol. 1, pp. 19-33, 2013, [Online]. Available: https://www.mathnet.ru/eng/ivpnz428.

[21] A. Bourchtein and L. Bourchtein, "On iterated Crank-Nicolson methods for hyperbolic and parabolic equations," Comput. Phys. Commun., vol. 181, no. 7, pp. 1242-1250, 2010, [Online]. Available: https://doi.org/10.1016/j.cpc.2010.03.011.

[22] H. Li et al., "Hamiltonian conserved Crank-Nicolson schemes for a semi-linear wave equation based on the exponential scalar auxiliary variables approach," Electron. Res. Arch. (ERA), vol. 32, no. 7, pp. 4433-4453, 2024, [Online]. Available: https://doi.org/10.3934/era.2024200.

[23] M. J. Huntul and M. Tamsir, "Identifying an unknown potential term in the fourth-order Boussinesq-Love equation from mass measurement," Eng. Comput., vol. 38, no. 10, pp. 3944-3968, 2021, [Online]. Available: https://doi.org/10.1108/EC-12-2020-0757.

[24] R. C. Mittal and R. K. Jain, "B-splines methods with redefined basis functions for solving fourth order parabolic partial differential equations," Appl. Math. Comput., vol. 217, no. 23, pp. 9741-9755, 2011, [Online]. Available: https://doi.org/10.1016/j.amc.2011.04.061.

[25] B. H. Dennis, G. S. Dulikravich, and S. Yoshimura, "A finite element formulation for the determination of unknown boundary conditions for three-dimensional steady thermoelastic problems," J. Heat Transf., vol. 126, no. 1, pp. 110-118, Feb. 2004, [Online]. Available: https://doi.org/10.1115/1.1640360.

[26] MathWorks, "Documentation: Optimization Toolbox - Least Squares (Model Fitting) Algorithms," 2026, [Online]. Available: https://www.mathworks.com.